Available online at www.sciencedirect.com

SciVerse ScienceDirect

Ceramics International 38 (2012) 6591–6597

CERAMICS INTERNATIONAL

www.elsevier.com/locate/ceramint

Electrochemical characteristics of cobalt-substituted lithium nickel oxides synthesized from lithium hydro-oxide and nickel and cobalt oxides

Myoung Youp Song[a,*], Ho Rim[b], Hye Ryoung Park[c]

[a]*Division of Advanced Materials Engineering, Hydrogen & Fuel Cell Research Center, Engineering Research Institute, Chonbuk National University, 567 Baekje-daero, Deokjin-gu Jeonju 561-756, Republic of Korea*

[b]*ASE Korea, 494 Munbal-dong, Paju-si, Gyeonggi-do 413-790, Republic of Korea*

[c]*School of Applied Chemical Engineering, Chonnam National University, 300 Yongbong-dong, Buk-gu Gwangju 500-757, Republic of Korea*

Received 2 May 2012; received in revised form 14 May 2012; accepted 14 May 2012
Available online 1 June 2012

Abstract

$LiNi_{1-y}Co_yO_2$ ($y=0.1$, 0.3 and 0.5) were synthesized by solid state reaction method at 800 °C and 850 °C from $LiOH \cdot H_2O$, NiO and Co_3O_4 as starting materials. The electrochemical properties of the synthesized $LiNi_{1-y}Co_yO_2$ were investigated. As the content of Co decreases, particle size decreases rapidly and particle size distribution gets more homogeneous. When the particle size is compared at the same composition, the particles synthesized at 850 °C are larger than those synthesized at 800 °C. $LiNi_{0.7}Co_{0.3}O_2$ synthesized at 850 °C has the largest intercalated and deintercalated Li quantity Δx among $LiNi_{1-y}Co_yO_2$ ($y=0.1$, 0.3 and 0.5). $LiNi_{0.7}Co_{0.3}O_2$ synthesized at 850 °C has the largest first discharge capacity (178 mAh/g), followed by $LiNi_{0.7}Co_{0.3}O_2$ (162 mAh/g) synthesized at 800 °C. $LiNi_{0.7}Co_{0.3}O_2$ synthesized at 800 °C has discharge capacities of 162 and 125 mAh/g at $n=1$ and $n=5$, respectively.

Keywords: $LiNi_{1-y}Co_yO_2$; Solid state reaction method; Voltage vs. x in $Li_xNi_{1-y}Co_yO_2$ curve; Discharge capacity

1. Introduction

Many researchers have investigated transition metal oxides such as $LiCoO_2$ [1–5], $LiNiO_2$ [6–13], and $LiMn_2O_4$ [14–20] as cathode materials for lithium secondary batteries [21]. $LiMn_2O_4$ is relatively cheap and does not cause environmental pollution, but its cycling performance is poor. $LiCoO_2$ has a large diffusivity and a high operating voltage, and it can be easily prepared. However, it has a disadvantage that it contains an expensive element, Co.

$LiNiO_2$ is a very promising cathode material since it has a large discharge capacity [22] and is relatively excellent from the viewpoints of economics and environment. However, due to the similar sizes of Li and Ni ($Li^+=0.72$ Å and $Ni^{2+}=0.69$ Å), the $LiNiO_2$ is practically obtained in the non-stoichiometric compositions, $Li_{1-y}Ni_{1+y}O_2$ [23,24], and the Ni^{2+} ions in the lithium planes obstruct the movement of the Li^+ ions during charge and discharge [25,26].

By incorporating $LiCoO_2$ and $LiNiO_2$ phases with $LiNi_{1-y}Co_yO_2$ compositions, the shortcomings of $LiCoO_2$ and $LiNiO_2$ can be remedied because the presence of cobalt stabilizes the structure in a strictly two-dimensional fashion, thus favoring good reversibility of the intercalation and deintercalation reactions [25,27–39]. Rougier et al. [25] reported that the stabilization of the two-dimensional character of the structure by cobalt substitution in $LiNiO_2$ is correlated with an increase in the cell performance, due to the decrease in the amount of extra-nickel ions in the inter-slab space which impede the lithium diffusion. Kang et al. [39] investigated the structure and electrochemical properties of the $Li_xCo_yNi_{1-y}O_2$ ($y=0.1$, 0.3, 0.5, 0.7 and 1.0) system synthesized by solid state reaction with various starting materials to optimize the characteristics and synthetic

*Corresponding author. Tel.: +82 63 270 2379; fax: +82 63 270 2386.
E-mail address: songmy@jbnu.ac.kr (M.Y. Song).

0272-8842/$36.00
http://dx.doi.org/10.1016/j.ceramint.2012.05.044

conditions of the $Li_xCo_yNi_{1-y}O_2$. The first discharge capacities of $Li_xCo_yNi_{1-y}O_2$ were 60–180 mAh/g depending on synthesis conditions.

Several methods are reported to synthesize $LiNiO_2$ and $LiNi_{1-y}Co_yO_2$, such as solid-state reaction method [40,41], coprecipitation method [42], sol–gel method [43], ultrasonic spray pyrolysis method [44], combustion method [11], and emulsion method [45]. In this work, solid state reaction method, which is quite simple, was used.

Researchers used different starting materials to synthesize $LiNi_{1-y}Co_yO_2$ by the solid-state reaction method [25,27–30,32–34,38,39,46]. $LiOH \cdot H_2O$ or Li_2CO_3, NiO or $NiCO_3$, and Co_3O_4 or $CoCO_3$ have been used as starting materials by some researchers [39,46] in order to synthesize $LiNi_{1-y}Co_yO_2$ by the solid-state reaction method.

In this work, $LiNi_{1-y}Co_yO_2$ ($y=0.1$, 0.3 and 0.5) cathode materials were synthesized by solid state reaction method at different temperatures using $LiOH \cdot H_2O$ as a source of Li, NiO as a source of Ni, and Co_3O_4 as a source of Co as starting materials. The electrochemical properties of the synthesized samples were then investigated. Structures of the synthesized $LiNi_{1-y}Co_yO_2$ ($y=0.1$, 0.3 and 0.5) were analyzed. Microstructures of the samples were observed. Voltage vs. x in $Li_xNi_{1-y}Co_yO_2$ curves for first charge–discharge and intercalated and deintercalated Li quantity Δx were studied. Destruction of unstable 3b sites and phase transitions were discussed from the first and second charge–discharge voltage vs. x in $LiNi_{0.7}Co_{0.3}O_2$ curves.

2. Experimental

$LiOH \cdot H_2O$, NiO and Co_3O_4 were used as starting materials in order to synthesize $LiNi_{1-y}Co_yO_2$ by the solid-state reaction method. All the starting materials (with the purity 99.9%) were purchased from Aldrich Co.

The experimental procedure for $LiNi_{1-y}Co_yO_2$ synthesis from $LiOH \cdot H_2O$, NiO and Co_3O_4 and characterization is given schematically in Fig. 1. The mixture of starting materials in the compositions of $LiNi_{1-y}Co_yO_2$ ($y=0.1$, 0.3 and 0.5) was mixed sufficiently and pelletized. This pellet was heat treated in air at 650 °C for 20 h. It was then ground, mixed, pelletized and calcined at 800 °C or 850 °C for 20 h. This pellet was cooled at a cooling rate 50 °C/min, ground, mixed and again pelletized. It was then calcined again at 800 °C or 850 °C for 20 h.

The phase identification of the synthesized samples was carried out by X-Ray Diffraction (XRD) analysis using Cu K_α radiation (Mac-Science Co., Ltd.). The scanning rate was 16°/min and the scanning range of diffraction angle (2θ) is $10° \le 2\theta \le 70°$. The morphologies of the samples were observed using a scanning electron microscope (SEM).

The electrochemical cells consisted of $LiNi_{1-y}Co_yO_2$ as a positive electrode, Li foil as a negative electrode, and electrolyte of 1 M $LiPF_6$ in a 1:1 (volume ratio) mixture of Ethylene Carbonate (EC) and Dimethyl Carbonate (DMC). A Whatman glass-fiber was used as the separator. The cells were assembled in an argon-filled dry box.

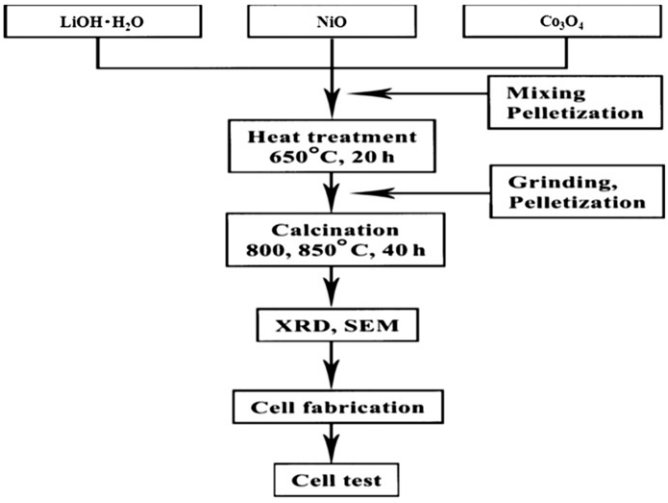

Fig. 1. Experimental procedure for $LiNi_{1-y}Co_yO_2$ synthesis from $LiOH \cdot H_2O$, NiO and Co_3O_4 and characterization.

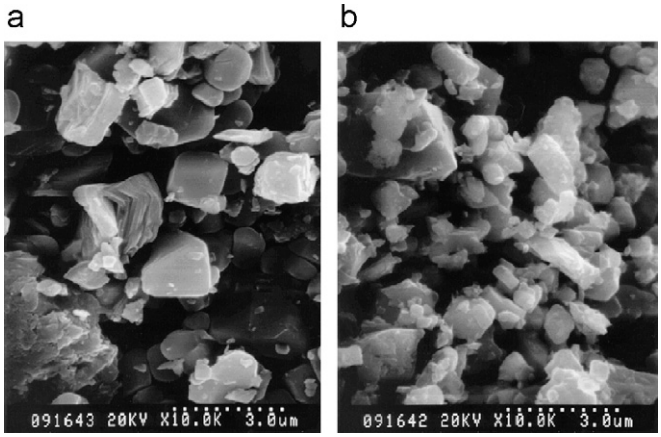

Fig. 2. SEM micrographs of $LiNi_{1-y}Co_yO_2$ synthesized from $LiOH \cdot H_2O$, NiO and Co_3O_4 at 800 °C; (a) $y=0.5$ and (b) $y=0.3$.

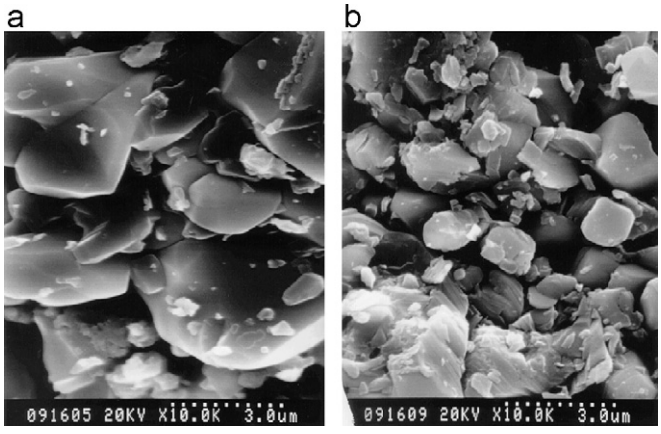

Fig. 3. SEM micrographs of $LiNi_{1-y}Co_yO_2$ synthesized from $LiOH \cdot H_2O$, NiO and Co_3O_4 at 850 °C; (a) $y=0.5$ and (b) $y=0.3$.

To fabricate the positive electrode, 89 wt% synthesized oxide, 10 wt% acetylene black, and 1 wt% Polytetrafluoroethylene (PTFE) binder were mixed in an agate mortar.

By introducing Li metal, Whatman glass-fiber, positive electrode, and the electrolyte, the cell was assembled. All the electrochemical tests were performed at room temperature with a potentiostatic/galvanostatic system (Mac-Pile system, Bio-Logic Co. Ltd.). The cells were cycled at a current density of 200 μA/cm^2 in a voltage range of 3.2–4.3 V.

3. Results and discussion

XRD patterns of $LiNi_{1-y}Co_yO_2$ (y=0.1, 0.3 and 0.5) powders calcined at 800 °C or 850 °C for 40 h using $LiOH \cdot H_2O$, NiO and Co_3O_4 as starting materials were identified as corresponding to a α-$NaFeO_2$ structure with a space group of $R\bar{3}m$.

SEM micrographs of $LiNi_{1-y}Co_yO_2$ (y=0.3 and 0.5) synthesized from $LiOH \cdot H_2O$, NiO and Co_3O_4 at 800 °C are shown in Fig. 2. As the content of Co decreases, particle size decreases rapidly and particle size distribution gets more homogeneous.

Fig. 3 exhibits SEM micrographs of $LiNi_{1-y}Co_yO_2$ (y=0.3 and 0.5) synthesized from $LiOH \cdot H_2O$, NiO and Co_3O_4 at 850 °C. The particles of $LiNi_{0.5}Co_{0.5}O_2$ are quite large. As the content of Co decreases, particle size decreases rapidly and particle size distribution gets more homogeneous. When the particle size is compared at the same composition, the particles synthesized at 850 °C are larger than those synthesized at 800 °C.

Voltage vs. x in $Li_xNi_{1-y}Co_yO_2$ curves for the first charge–discharge of $LiNi_{1-y}Co_yO_2$ synthesized at 800 °C and 850 °C are shown in Fig. 4. Among $LiNi_{1-y}Co_yO_2$ (y=0.1, 0.3 and 0.5) synthesized at 800 °C, $LiNi_{0.7}Co_{0.3}O_2$ has the largest intercalated and deintercalated Li quantity Δx, followed in order by $LiNi_{0.9}Co_{0.1}O_2$ and $LiNi_{0.5}Co_{0.5}O_2$.

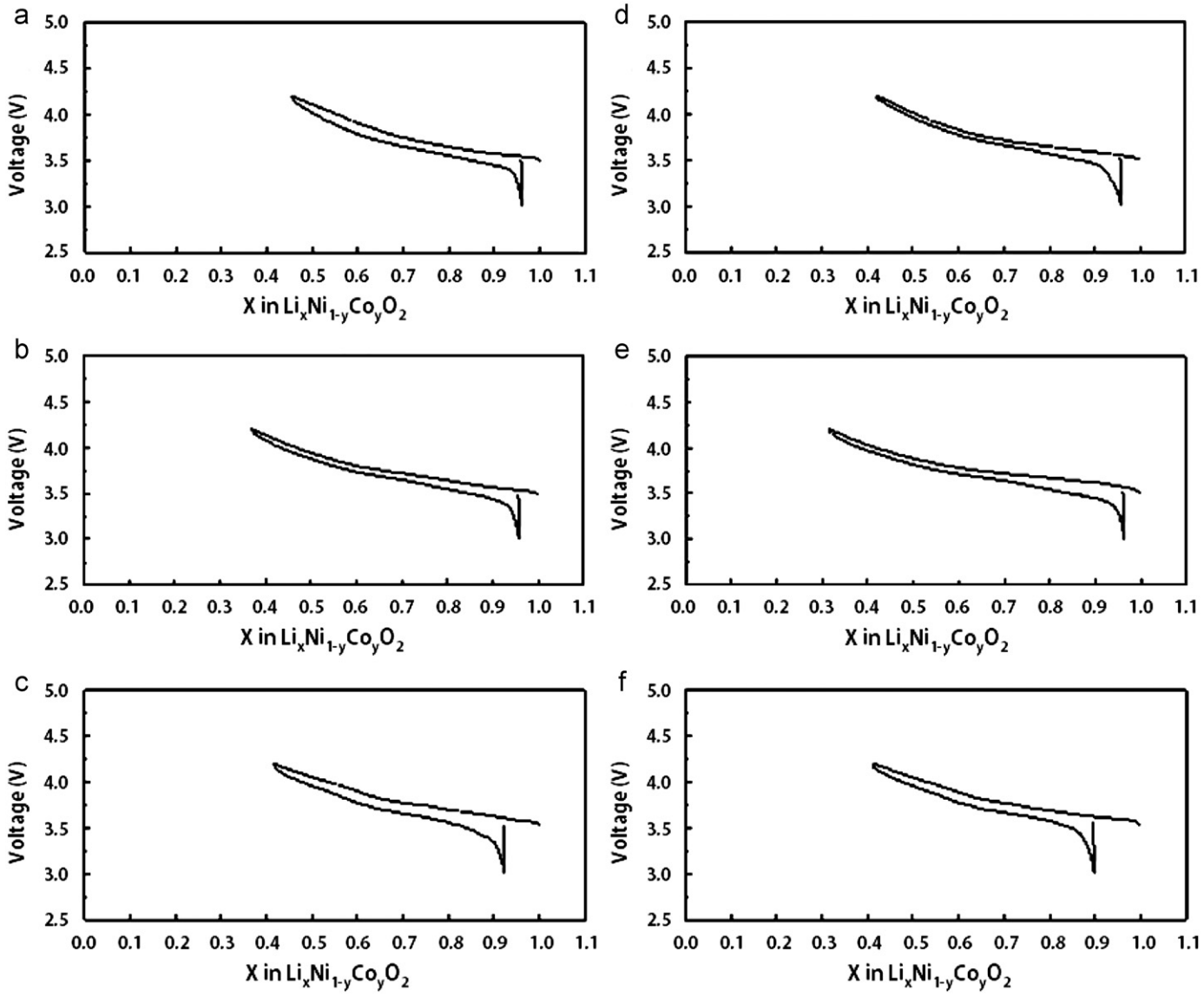

Fig. 4. Voltage vs. x in $Li_xNi_{1-y}Co_yO_2$ curves at a current density of 200 μA/cm^2 for the first charge–discharge of $LiNi_{1-y}Co_yO_2$ synthesized at 800 °C; (a) y=0.5, (b) y=0.3, and (c) y=0.1, and at 850 °C; (d) y=0.5, (e) y=0.3, and (f) y=0.1.

Among $LiNi_{1-y}Co_yO_2$ (y=0.1, 0.3 and 0.5) synthesized at 850 °C, $LiNi_{0.7}Co_{0.3}O_2$ has the largest intercalated and deintercalated Li quantity Δx, followed in order by $LiNi_{0.5}Co_{0.5}O_2$ and $LiNi_{0.9}Co_{0.1}O_2$.

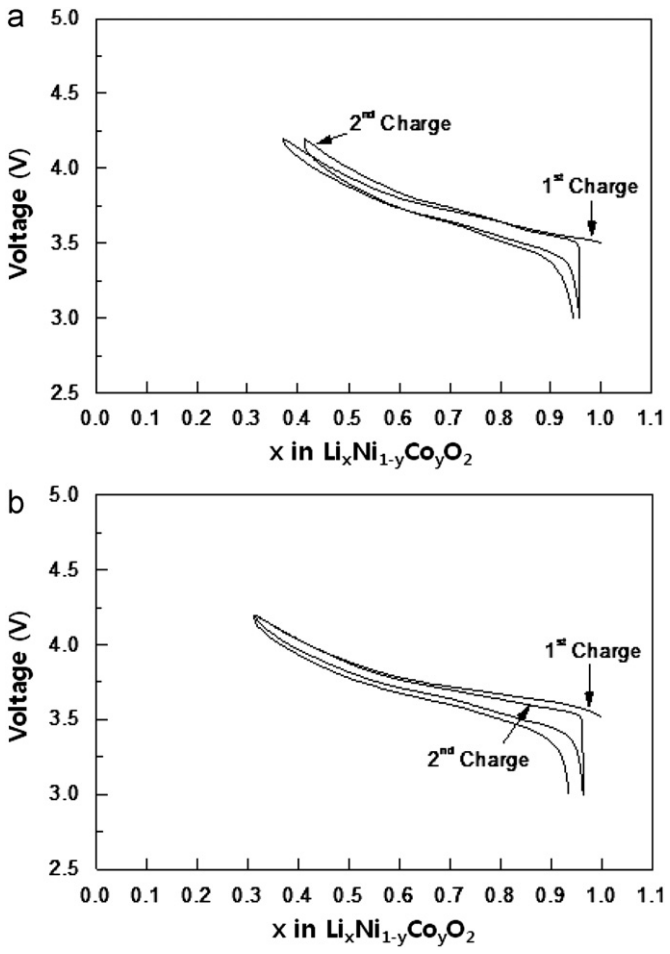

Fig. 5. Voltage vs. x in $Li_xNi_{1-y}Co_yO_2$ curves for the first and second charge–discharge of $LiNi_{0.7}Co_{0.3}O_2$ synthesized (a) at 800 °C, and (b) at 850 °C.

$LiNi_{0.7}Co_{0.3}O_2$ shows the best intercalation and deintercalation reactions among $LiNi_{1-y}Co_yO_2$ (y=0.1, 0.3 and 0.5). Fig .5 presents voltage vs. x in $Li_xNi_{1-y}Co_yO_2$ curves for the first and second charge–discharge of $LiNi_{0.7}Co_{0.3}O_2$ synthesized at 800 °C and 850 °C. The $LiNi_{0.7}Co_{0.3}O_2$ synthesized at 850 °C shows the value of Δx closer to that of the first cycle, compared with the $LiNi_{0.7}Co_{0.3}O_2$ synthesized at 800 °C.

First charge capacities at a current density of 200 μA/cm^2 in the voltage range of 3.0–4.3 V for $LiNi_{1-y}Co_yO_2$ synthesized at 800 °C and at 850 °C are shown in Fig. 6. $LiNi_{0.7}Co_{0.3}O_2$ synthesized at 850 °C has the largest first discharge capacity, followed in order by $LiNi_{0.7}Co_{0.3}O_2$ synthesized at 800 °C, $LiNi_{0.5}Co_{0.5}O_2$ synthesized at 850 °C, $LiNi_{0.9}Co_{0.1}O_2$ synthesized at 800 °C, $LiNi_{0.5}Co_{0.5}O_2$ synthesized at 800 °C, and $LiNi_{0.9}Co_{0.1}O_2$ synthesized at 850 °C.

Fig. 7 presents the variations of the first charge capacity with the value of y for $LiNi_{1-y}Co_yO_2$ synthesized at 800 °C and 850 °C. When the first discharge capacities of $LiNi_{1-y}Co_yO_2$ (y=0.1, 0.3 and 0.5) synthesized at 800 °C or 850 °C are compared, $LiNi_{0.7}Co_{0.3}O_2$ has larger first discharge capacity than $LiNi_{0.5}Co_{0.5}O_2$ and $LiNi_{0.9}Co_{0.1}O_2$. $LiNi_{0.7}Co_{0.3}O_2$ synthesized at 850 °C has the largest first discharge capacity (178 mAh/g), followed in order by $LiNi_{0.7}Co_{0.3}O_2$ (162 mAh/g) synthesized at 800 °C, $LiNi_{0.5}Co_{0.5}O_2$ (148 mAh/g) synthesized at 850 °C, $LiNi_{0.9}Co_{0.1}O_2$ (140 mAh/g) synthesized at 800 °C, $LiNi_{0.5}Co_{0.5}O_2$ (139 mAh/g) synthesized at 800 °C, and $LiNi_{0.9}Co_{0.1}O_2$ (134 mAh/g) synthesized at 850 °C.

The variations of discharge capacity with number of cycles for $LiNi_{0.5}Co_{0.5}O_2$ and $LiNi_{0.7}Co_{0.3}O_2$ synthesized at 800 °C are shown in Fig. 8. $LiNi_{0.5}Co_{0.5}O_2$ has better cycling performance than $LiNi_{0.7}Co_{0.3}O_2$. $LiNi_{0.5}Co_{0.5}O_2$

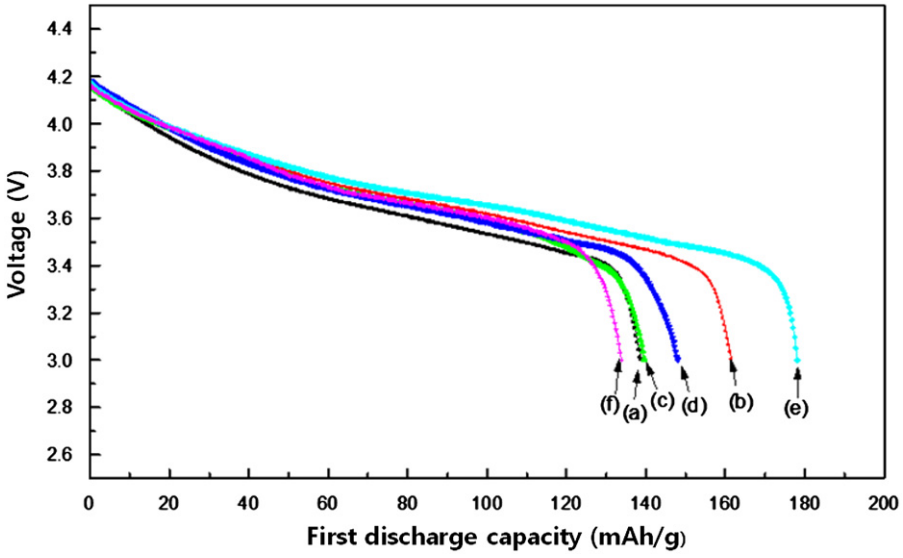

Fig. 6. First charge capacities at a current density of 200 μA/cm^2 in the voltage range of 3.0–4.3 V for $LiNi_{1-y}Co_yO_2$ synthesized at 800 °C; (a) y=0.5, (b) y=0.3, and (c) y=0.1, and at 850 °C; (d) y=0.5, (e) y=0.3, and (f) y=0.1.

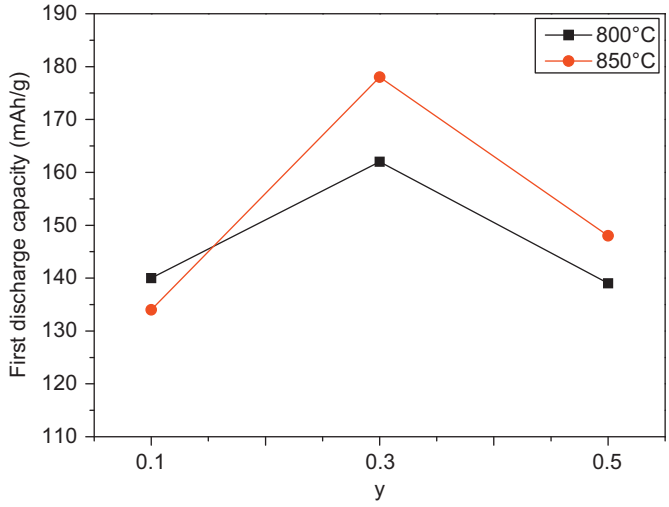

Fig. 7. Variations of the first discharge capacity with value of y for $LiNi_{1-y}Co_yO_2$ synthesized at 800 °C and 850 °C.

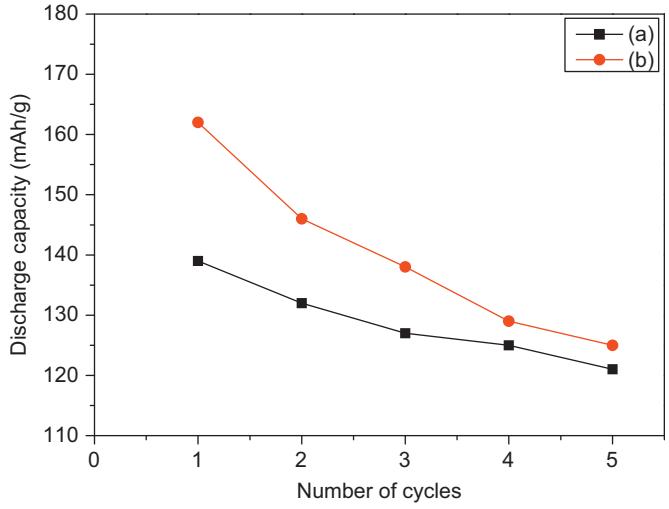

Fig. 8. Variations of discharge capacity with number of cycles for $LiNi_{1-y}Co_yO_2$ synthesized at 800 °C; (a) $y=0.5$, and (b) $y=0.3$.

has discharge capacities of 139 and 121 mAh/g at $n=1$ and $n=5$, respectively. $LiNi_{0.7}Co_{0.3}O_2$ has discharge capacities of 162 and 125 mAh/g at $n=1$ and $n=5$, respectively.

The voltage vs. x in $Li_xNi_{1-y}Co_yO_2$ curves at a current density of 200 μA/cm^2 for the first charge–discharge of $LiNi_{1-y}Co_yO_2$ in Fig. 4 show that, as compared with the quantity of the deintercalated Li ions by the first charging, that of the intercalated Li ions by the first discharging is much smaller, which is revealed by the difference in Δx of the first charge and discharge curves, for all the samples. The lengths of plateaus in the charge and discharge curves are proportional to charge and discharge capacities. During the first charging, Li ions deintercalate not only from stable 3b sites but also from unstable 3b sites. After deintercalation from unstable 3b sites, the unstable 3b sites will be destroyed. This is considered to lead to smaller quantity of the intercalated Li ions by the first discharging than that of the deintercalated Li ions by the first charging.

The voltage vs. x in $Li_xNi_{1-y}Co_yO_2$ curves for the first and second charge–discharge of $LiNi_{0.7}Co_{0.3}O_2$ synthesized at 800 °C, and at 850 °C in Fig. 5 show that the difference in Δx of the second charge and discharge curves is smaller than that of the first charge and discharge curves. This shows that destruction of unstable 3b sites occurs less severely at the second cycle than at the first cycle.

In the voltage vs. x in $Li_xNi_{1-y}Co_yO_2$ curves for the first and second charge–discharge of $LiNi_{0.7}Co_{0.3}O_2$ synthesized at 800 °C and 850 °C in Fig. 5, the charge–discharge curves exhibit quite long plateaus, where two phases coexist [47]. Arai et al. [48] reported that, during charging and discharging, $LiNiO_2$ goes through three phase transitions; phase transitions from hexagonal structure (H1) to monoclinic structure (M), from monoclinic structure (M) to hexagonal structure (H2), and from hexagonal structure (H2) to hexagonal structure (H3) or vice versa. Ohzuku et al. [40] reported that, during charging and discharging, $LiNiO_2$ goes through four phase transitions; phase transitions from H1 to M, from M to H2, from H2 to hexagonal structures H2+H3, and from H2+H3 to H3 or vice versa. Song et al. [49] reported that $-dx/|dV|$ vs. V curves of $LiNi_{1-y}Ti_yO_2$ ($y=0.012$ and 0.025) for charging and discharging showed four peaks, revealing the four phase transitions from H1 to M, from M to H2, from H2 to H2+H3, and from H2+H3 to H3 or vice versa.

4. Conclusions

As the content of Co decreases, particle size decreases rapidly and particle size distribution gets more homogeneous. When the particle size is compared at the same composition, the particles synthesized at 850 °C are larger than those synthesized at 800 °C. When the first discharge capacities of $LiNi_{1-y}Co_yO_2$ ($y=0.1$, 0.3 and 0.5) synthesized at 800 °C or 850 °C are compared, $LiNi_{0.7}Co_{0.3}O_2$ has larger first discharge capacity than $LiNi_{0.5}Co_{0.5}O_2$ and $LiNi_{0.9}Co_{0.1}O_2$. $LiNi_{0.7}Co_{0.3}O_2$ has the largest intercalated and deintercalated Li quantity Δx among $LiNi_{1-y}Co_yO_2$ ($y=0.1$, 0.3 and 0.5). The $LiNi_{0.7}Co_{0.3}O_2$ synthesized at 850 °C has the largest first discharge capacity (178 mAh/g), followed in order by $LiNi_{0.7}Co_{0.3}O_2$ (162 mAh/g) synthesized at 800 °C, and $LiNi_{0.5}Co_{0.5}O_2$ (148 mAh/g) synthesized at 850 °C.

References

[1] K. Ozawa, Lithium-ion rechargeable batteries with $LiCoO_2$ and carbon electrodes: the $LiCoO_2$/C system, Solid State Ionics 69 (1994) 212–221.
[2] R. Alcántara, P. Lavela, J.L. Tirado, R. Stoyanova, E. Zhecheva, Structure and electrochemical properties of boron-doped $LiCoO_2$, Journal of Solid State Chemistry 134 (1997) 265–273.
[3] Z.S. Peng, C.R. Wan, C.Y. Jiang, Synthesis by sol–gel process and characterization of $LiCoO_2$ cathode materials, Journal of Power Sources 72 (1998) 215–220.

[4] S.K. Kim, D.H. Yang, J.S. Sohn, Y.C. Jung, Resynthesis of $LiCo_{1-x}Mn_xO_2$ as a cathode material for lithium secondary batteries, Metals and Materials International 18 (2) (2012) 321–326.
[5] W.D. Yang, C.Y. Hsieh, H.J. Chuang, Y.S. Chen, Preparation and characterization of nanometric-sized $LiCoO_2$ cathode materials for lithium batteries by a novel sol–gel method, Ceramics International 36 (1) (2010) 135–140.
[6] J.R. Dahn, U. von Sacken, C.A. Michal, Structure and electrochemistry of $Li_{1\pm y}NiO_2$ and a new Li_2NiO_2 phase with the $Ni(OH)_2$ structure, Solid State Ionics 44 (1990) 87–97.
[7] J.R. Dahn, U. von Sacken, M.W. Juzkow, H. Al-Janaby, Rechargeable $LiNiO_2$/carbon cells, Journal of the Electrochemical Society 138 (1991) 2207–2212.
[8] H.U. Kim, D.R. Mumm, H.R. Park, M.Y. Song, Synthesis by a simple combustion method and electrochemical properties of $LiCo_{1/3}Ni_{1/3}Mn_{1/3}O_2$, Electronic Materials Letters 6 (3) (2010) 91–95.
[9] S.H. Ju, J.H. Kim, Y.C. Kang, Electrochemical properties of $LiNi_{0.8}Co_{0.2-x}Al_xO_2$ $(0 \le x \le 0.1)$ cathode particles prepared by spray pyrolysis from the spray solutions with and without organic additives, Metals and Materials International 16 (2) (2010) 299–303.
[10] D.H. Kim, Y.U. Jeong, D.H. Kim, Y.U. Jeong, Crystal structures and electrochemical properties of $LiNi_{1-x}Mg_xO_2$ $(0 \le x \le 0.1)$ for cathode materials of secondary lithium batteries, Korean Journal of Metals and Materials 48 (3) (2010) 262–267.
[11] S.N. Kwon, J.H. Song, D.R. Mumm, Effects of cathode fabrication conditions and cycling on the electrochemical performance of $LiNiO_2$ synthesized by combustion and calcination, Ceramics International 37 (5) (2011) 1543–1548.
[12] M.Y. Song, C.K. Park, H.R. Park, D.R. Mumm, Variations in the electrochemical properties of metallic elements-substituted $LiNiO_2$ cathodes with preparation and cathode fabrication conditions, Electronic Materials Letters 8 (1) (2012) 37–42.
[13] M.Y. Song, D.R. Mumm, C.K. Park, H.R. Park, Cycling performances of LiNi 1− y M y O2 (M=Ni, Ga, Al and/or Ti) synthesized by wet milling and solid-state method, Metals and Materials International 18 (3) (2012) 465–472.
[14] J.M. Tarascon, E. Wang, F.K. Shokoohi, W.R. Mckinnon, S. Colson, The spinel phase of $LiMn_2O_4$ as a cathode in secondary lithium cells, Journal of the Electrochemical Society 138 (1991) 2859–2864.
[15] A.R. Armstrong, P.G. Bruce, Synthesis of layered $LiMnO_2$ as an electrode for rechargeable lithium batteries, Nature 381 (1996) 499–500.
[16] M.Y. Song, D.S. Ahn, On the capacity deterioration of Spinel phase $LiMn_2O_4$ with cycling around 4 V, Solid State Ionics 112 (1998) 21–24.
[17] M.Y. Song, D.S. Ahn, H.R. Park, Capacity fading of spinel phase $LiMn_2O_4$ with cycling, Journal of Power Sources 83 (1999) 57–60.
[18] D.S. Ahn, M.Y. Song, Variations of the electrochemica properties of $LiMn_2O_4$ with synthesis conditions, Journal of the Electrochemical Society 147 (3) (2000) 874–879.
[19] H.J. Guo, Q.H. Li, X.H. Li, Z.X. Wang, W.J. Peng, Novel synthesis of $LiMn_2O_4$ with large tap density by oxidation of manganese powder, Energy Conversion and Management 52 (4) (2011) 2009–2014.
[20] C. Wan, M. Cheng, D. Wu, Synthesis of spherical spinel $LiMn_2O_4$ with commercial manganese carbonate, Powder Technology 210 (1) (2011) 47–51.
[21] J.W. Park, J.H. Yu, K.W. Kim, H.S. Ryu, J.H. Ahn, C.S. Jin, K.H. Shin, Y.C. Kim, H.J. Ahn, Surface morphology changes of lithium/sulfur battery using multi-walled carbon nanotube added sulfur electrode during cyclings, Korean Journal of Metals and Materials 49 (2) (2011) 174–179.
[22] Y. Nishida, K. Nakane, T. Satoh, Synthesis and properties of gallium-doped $LiNiO_2$ as the cathode material for lithium secondary batteries, Journal of Power Sources 68 (1997) 561–564.
[23] P. Barboux, J.M. Tarascon, F.K. Shokoohi, The use of acetates as precursors for the low-temperature synthesis of $LiMn_2O_4$ and $LiCoO_2$ intercalation compounds, Journal of Solid State Chemistry 94 (1991) 185–196.
[24] J. Morales, C. Perez-Vicente, J.L. Tirado, Cation distribution and chemical deintercalation of $Li_{1-x}Ni_{1+x}O_2$, Materials Research Bulletin 25 (1990) 623–630.
[25] A. Rougier, I. Saadoune, P. Gravereau, P. Willmann, C. Delmas, Effect of cobalt substitution on cationic distribution in $LiNi_{1-y}Co_yO_2$ electrode materials, Solid State Ionics 90 (1996) 83–90.
[26] B.J. Neudecker, R.A. Zuhr, B.S. Kwak, J.B. Bates, J.D. Robertson, Lithium manganese nickel oxides $Li_x(Mn_yNi_{1-y})_{2-x}O_2$, Journal of the Electrochemical Society 145 (1998) 4148–4157.
[27] C. Delmas, I. Saadoune, Electrochemical and physical properties of the $Li_xNi_{1-y}Co_yO_2$ phases, Solid State Ionics 53 (56) (1992) 370–375.
[28] E. Zhecheva, R. Stoyanova, Stabilization of the layered crystal structure of $LiNiO_2$ by Co-substitution, Solid State Ionics 66 (1993) 143–149.
[29] C. Delmas, I. Saadoune, A. Rougier, The cycling properties of the $Li_xNi_{1-y}CoyO_2$ electrode, Journal of Power Sources 43 (44) (1993) 595–602.
[30] A. Ueda, T. Ohzuku, Solid-state redox reactions of $LiNi_{1/2}Co_{1/2}O_2$ ($R\bar{3}m$) for 4 V secondary lithium cells, Journal of the Electrochemical Society 141 (1994) 2010–2014.
[31] M. Menetrier, A. Rougier, C. Delmas, Cobalt segregation in the $LiNi_{1-y}Co_yO_2$ solid solution: a preliminary ^{7}Li NMR study, Solid State Communications 90 (1994) 439–442.
[32] R. Alcantara, J. Morales, J.L. Tirado, R. Stoyanova, E. Zhecheva, Structure and electrochemical properties of $Li_{1-x}(Ni_yCo_{1-y})_{1+x}O_2$ effect of chemical delithiation at 0 °C, Journal of the Electrochemical Society 142 (1995) 3997–4005.
[33] B. Banov, J. Bourilkov, M. Mladenov, Cobalt stabilized layered lithium-nickel oxides, cathodes in lithium rechargeable cells, Journal of Power Sources 54 (1995) 268–270.
[34] Y.M. Choi, S.I. Pyun, S.I. Moon, Effects of cation mixing on the electrochemical lithium intercalation reaction into porous $Li_{1-\delta}Ni_{1-y}Co_yO_2$ electrodes, Solid State Ionics 89 (1996) 43–52.
[35] S.J. Lee, J.K. Lee, D.W. Kim, H.K. Baik, S.M. Lee, Fabrication of thin film $LiCo_{0.5}Ni_{0.5}O_2$ cathode for Li rechargeable microbattery, Journal of the Electrochemical Society 143 (1996) 268–270.
[36] D. Caurant, N. Baffier, B. Garcia, J.P. Pereira-Ramos, Synthesis by a soft chemistry route and characterization of $LiNi_xCo_{1-x}O_2$ $(0 \le x \le 1)$ cathode materials, Solid State Ionics 91 (1996) 45–54.
[37] K. Amine, H. Yasuda, Y. Fujita, New process for low temperature preparation of $LiNi_{1-x}Co_xO_2$. Cathode material for lithium cells, Les Annales de Chimie—Science des Matériaux 23 (1998) 37–42.
[38] C.C. Chang, N. Scarr, P.N. Kumta, Synthesis and electrochemical characterization of $LiMO_2$ (M=Ni, $Ni_{0.75}Co_{0.25}$) for rechargeable lithium ion batteries, Solid State Ionics 112 (1998) 329–344.
[39] S.G. Kang, K.S. Ryu, S.H. Chang, S.C. Park, The novel synthetic route to $LiCo_yNi_{1-y}O_2$ as a cathode material in lithium secondary batteries, Bulletin of the Korean Chemical Society 22 (12) (2001) 1328–1332.
[40] T. Ohzuku, A. Ueda, M. Nagayama, Electrochemistry and structural chemistry of $LiNiO_2$ ($R\bar{3}m$) for 4 V secondary lithium cells, Journal of the Electrochemical Society 140 (1993) 1862–1870.
[41] Z. Lu, X. Huang, H. Haung, L. Chen, J. Schoonman, The phase transition and optimal synthesis temperature of $LiNiO_2$, Solid State Ionics 120 (1999) 103–107.
[42] M. Guilmard, A. Rougier, M. Grune, L. Croguennec, C. Delmas, Effects of aluminum on the structural and electrochemical properties of $LiNiO_2$, Journal of Power Sources 115 (2003) 305–314.
[43] B.J. Hwang, R. Santhanam, C.H. Chen, Effect of synthesis conditions on electrochemical properties of $LiCo_yNi_{1-y}O_2$ cathode for lithium rechargeable batteries, Journal of Power Sources 114 (2003) 244–252.
[44] S.H. Park, C.S. Yoon, S.G. Kang, H.S. Kim, S.I. Moon, Y.K. Sun, Synthesis and structural characterization of layered Li $[Ni_{1/3}Co_{1/3}Mn_{1/3}]O_2$ cathode materials by ultrasonic spray pyrolysis method, Electrochimica Acta 49 (2004) 557–563.

[45] B.H. Kim, J.H. Kim, I.H. Kwon, M.Y. Song, Electrochemical properties of $LiNiO_2$ cathode material synthesized by the emulsion method, Ceramics International 33 (2007) 837–841.

[46] M.Y. Song, H. Rim, E. Bang, Electrochemical properties of cathode materials $LiNi_{1-y}Co_yO_2$ synthesized using various starting materials, Journal of Applied Electrochemistry 34 (2004) 383–389.

[47] W. Li, J.N. Reimers, J.R. Dahn, In situ x-ray diffraction and electrochemical studies of $Li_{1-x}NiO_2$, Solid State Ionics 67 (1993) 123–130.

[48] H. Arai, S. Okada, H. Ohtsuka, M. Ichimura, J. Yamaki, Characterization and cathode performance of $Li_{1-x}Ni_{1+x}O_2$ prepared with the excess lithium method, Solid State Ionics 80 (1995) 261–269.

[49] M.Y. Song, D.S. Lee, H.R. Park, Electrochemical properties of $LiNi_{1-y}Ti_yO_2$ and $LiNi_{0.975}M_{0.025}O_2$ (M = Zn, Al, and Ti) synthesized by the solid-state reaction method, Materials Research Bulletin 47 (2012) 1021–1027.